Make invisible visible: to the guaranteed signal averaging for the distributed fiber sensor

Make invisible visible: to the guaranteed signal averaging for the distributed fiber sensor

I A Ershov[1], O V Stukach[1,2], I B Tsydenzhapov[3], I V Sychev[3]
[1]Novosibirsk State Technical University, Novosibirsk, Russia
[2]National Research University Higher School of Economics, Moscow, Russia
[3]KEEPLINE R&D, Novosibirsk, Russia

Abstract. Fiber-optic sensors are becoming wide spreading in many fields due to a lot of advantages such as high spatial resolution, small size, immunity to the electromagnetic disturbances and possibility of multiplexing. Many benefits are fundamentally unattainable for electrical sensors by the physical operation principles. The processing of signals received from the optical fiber temperature sensor is considered. Raman sensor provides high spatial resolution. The main problem of signal processing for the temperature calculating is a large noise arising from the low level of current received from opto-converter. A method for estimating the additive noise level is presented based on calculation of the standard deviation. Comments concern the multiplicative noise during the rise and fall of the signal are given. Possibilities of guaranteed identification of DTS signals based on experimental measurement of statistical characteristics and representation it as so-called potential characteristic is evaluated. The signal-to-noise ratio may be increased by averaging the potential characteristics.

1. Introduction

Immunity to the electromagnetic field, small weight and size, possibility of multiplexing, and much more advantages make a fiber-optic sensor the most popular nowadays [1]. But the main advantage distinguishes this optic technology from all previous ones is the best spatial resolution along fiber length. It is fundamentally unattainable using conventional electronic measuring instruments [2]. In the case of conventional electronic sensors, it is necessary to use many sensing elements connected in a single tool. Optical fiber is used for direct measurement and information transmission. Thus, it is possible to achieve the highest spatial resolution, which can be used to solve many practical problems, for example, measuring temperature and small movements [3–4].

Sensors based on different principles are developed for use in various fields due to all these advantages. Fiber-optic sensors are used for chemical sensing or bio-sensing, pressure sensing, temperature, refractive index etc. [5–10]. Note the scope of their application has expanded in a relatively short period and continues to growing. The paper discusses results of measurements of the fiber optic temperature sensor. Today it is very popular to use a method of combining single mode fiber (SMF) and multi-mode fibers (MMF) [11]. This approach is actively modified using a few-mode fiber (FMF) conical shape [12] or a thin-diameter fiber (TDF) [13]. All these approaches are good in situations where it is necessary to temperature measure at short distance or at specific spatial point. In our experiments we use the Raman scattering sensor capable of temperature measuring along the fiber length, which is excellent for temperature measurements at long distances, such as gas pipelines [14]. The measurement system layout does not differ from the known ones [2, 8], and the experimental setup is shown in the photo in figure 1.

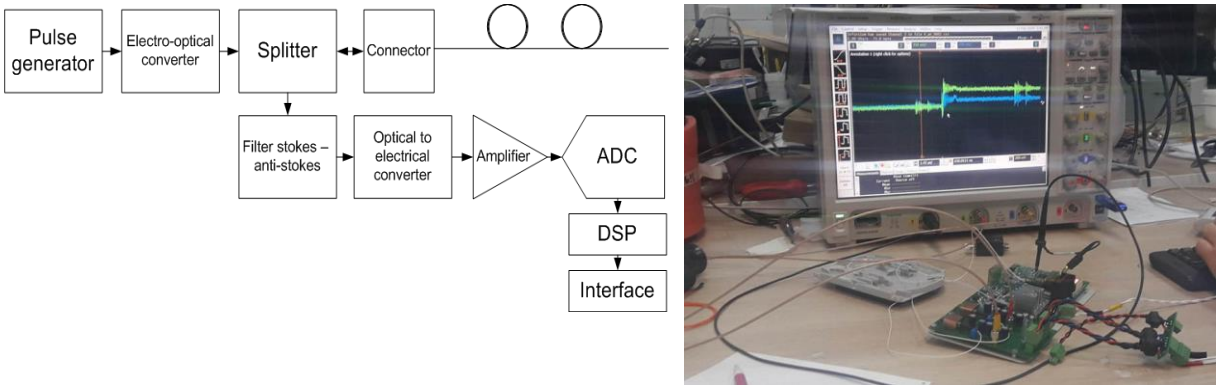

Figure 1. Circuit and photo of the measurement layout.

2. Problem statement

Temperature measurements using the optical fiber sensor are allied with the noise-like signal processing based on the physical principles of the optical fiber sensor operation [14]. The measurements are based on the Raman scattering effect. Back-reflected light has Stokes I_s and anti-Stokes I_{as} components, the intensity ratio of which depends on temperature T [2]:

$$R(T) = I_{as} / I_s. \quad (1)$$

The optical converter is installed on the same side of the fiber as the electron-optical converter to measure the amplitudes of the signals. Actually this signal is so weak due to large noise. Example of the anti-Stokes component is shown in figure 2.

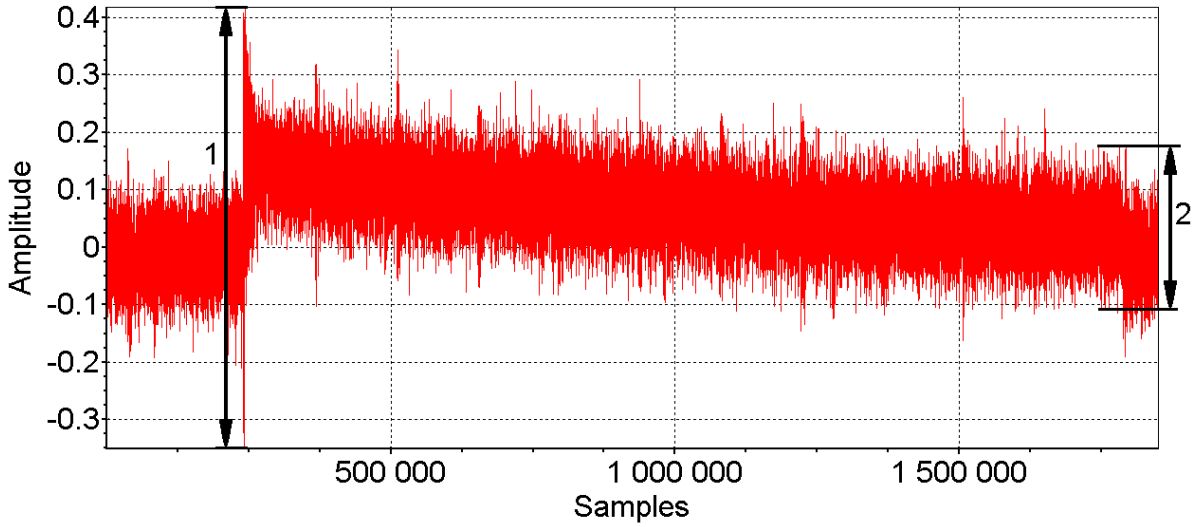

Figure 2. Anti-Stokes component with multiply (1) and additive (2) noise.

This graph shows the amplitude of the anti-Stokes component along all fiber length. A sharp increase (start time) and a sharp decline in the signal determine the operating domain of the graph. The signal contains additive and multiply noise. Multiply noise (1) arisen by a transient during a risetime and fall of the signal. The most significant effect is the transient during the risetime. Additive noise (2) is caused by many factors that have a continuous effect in the signal. As a result, the signal-to-noise ratio is very small, which is why the developed filtering methods do not operate well. Therefore, all hardware and software ways to increase the signal-to-noise ratio are of the practical interest. New signal processing methods should increase the accuracy and sensitivity of optical temperature sensors. In fact, we may reduce this problem to the problem of identification. Here the effect is not known, but measured statistical characteristics can be known.

3. Signal processing

First of all, it should be eliminate the transient process connected with the laser start and stochastic processes in the measuring device. It will make possible to evaluate the additive component of noise. Here reduction of the operational part is the most rational. It is almost impossible to completely exclude the transient process since it appears before the primary signal gain and amplifies with it. There are two transients, during risetime and falltime. The largest measurement error is caused by the transient with large amplitude during risetime, and the small amplitude transient in decline occurs after the operating area. Unlike other noises can be reduced by averaging, the transient during risetime is not level off.

Since we have a signal recording from a digital oscilloscope in the kind of two million samples, we remove the transient samples from variable. We use the standard deviation (SD) to assess the additive noise level. It is necessary to divide the data into groups of *S* samples. An utility was design and SD values were calculated for the selected *S* to determine the optimal number of samples in the group according to the maximum SD criterion (figure 3).

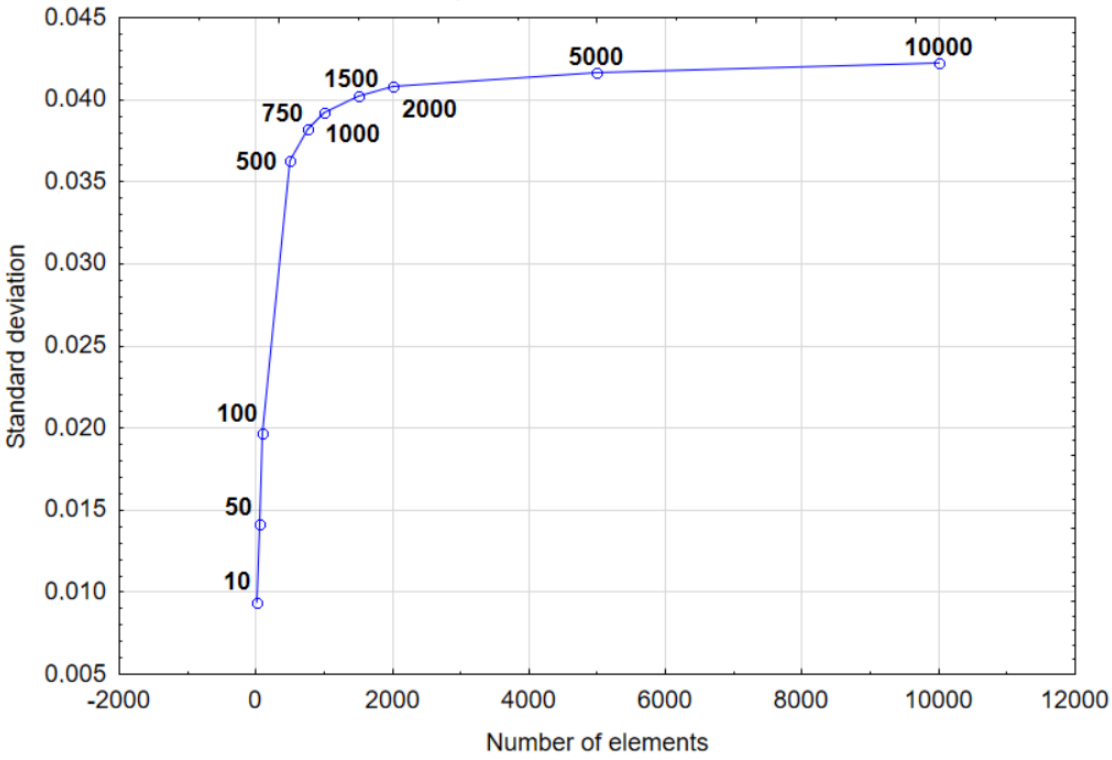

Figure 3. Dependence of the average SD on the number of samples in the group.

From figure 3 follows that at *S*=1000 the SD stop to increase noticeably. We carried out the SD diagram for each signal group along length of the optical fiber to check possibility of SD using for estimating the value of additive noise (figure 4).

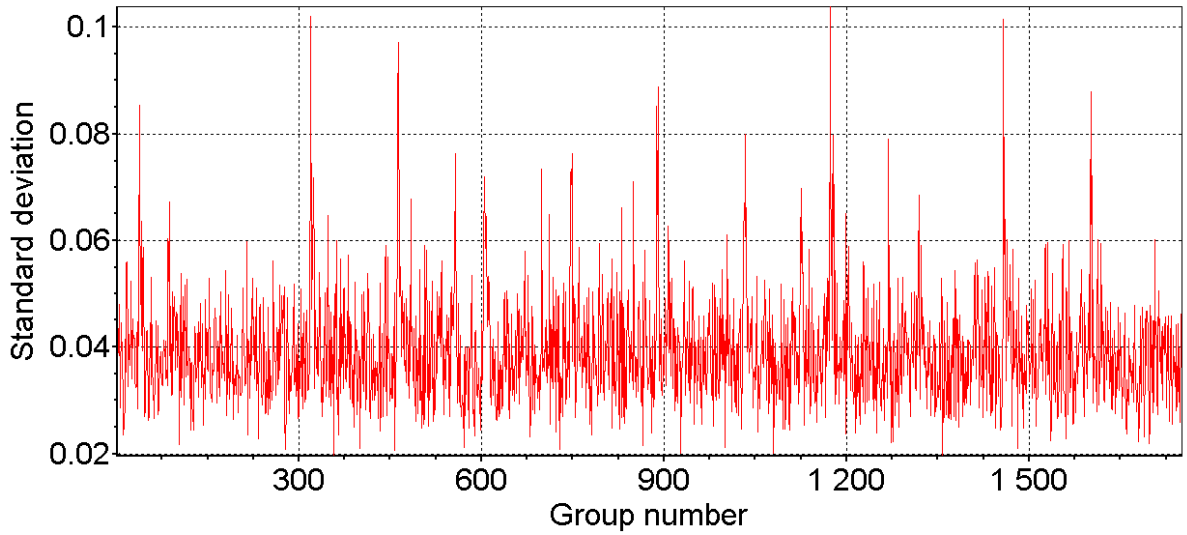

Figure 4. SD of each group.

All data were combined into 2000 groups. From figure 4 follows that most of the groups of samples have the close SD. Therefore, we can guess the average value of SD will be a reliable value for additive noise assessing. Non-periodic outliers on the graph in the abnormally large standard deviations mean that there are previously unknown causes of noise. Emissions will not have a significant effect to the mean for temperature calculation, since it amount in the variable is negligible. If we exclude them from the variable, we get unaccounted noise. In this case, the average of the SD is 0.0392 V.

Figure 5 shows the Stokes and anti-Stokes components at a temperature of 24.5 °C over all fiber length with averaging by 1024 variables of signal. The Stokes component on the chart is above the anti-Stokes component.

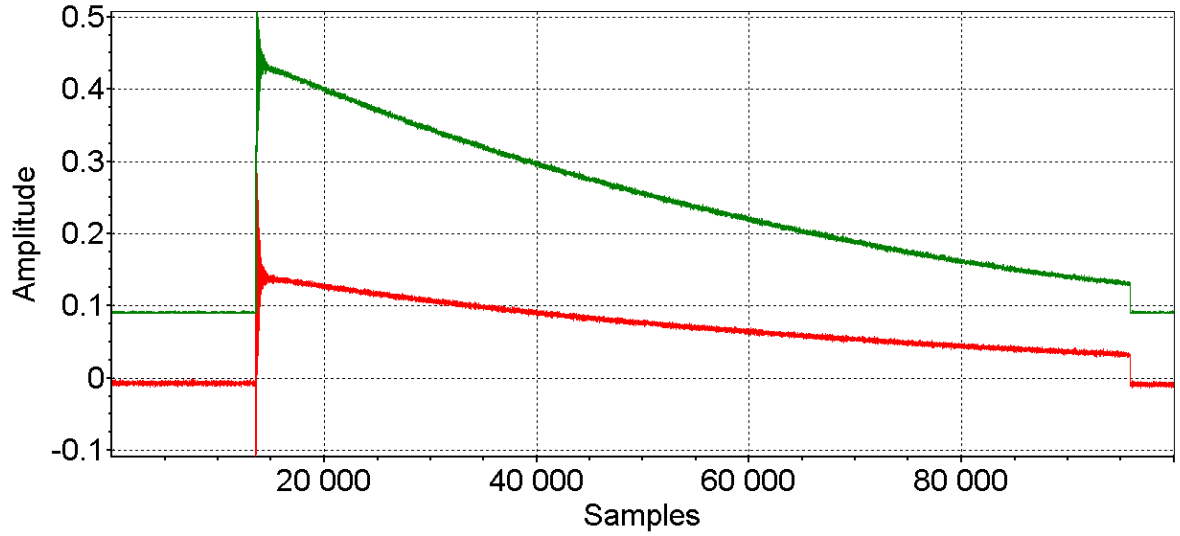

Figure 5. Stokes and anti-Stokes components at 24.5 °C.

Voltage in the corresponding section of the graph increases when part of the fiber is heated. Figure 6 shows the part of the graph that changed after heating to 97.2 °C. Place of heating is determined by start time from beginning of the optical signal to the light effected the opto-converter and light velocity. Here we can measure the temperature along all fiber length.

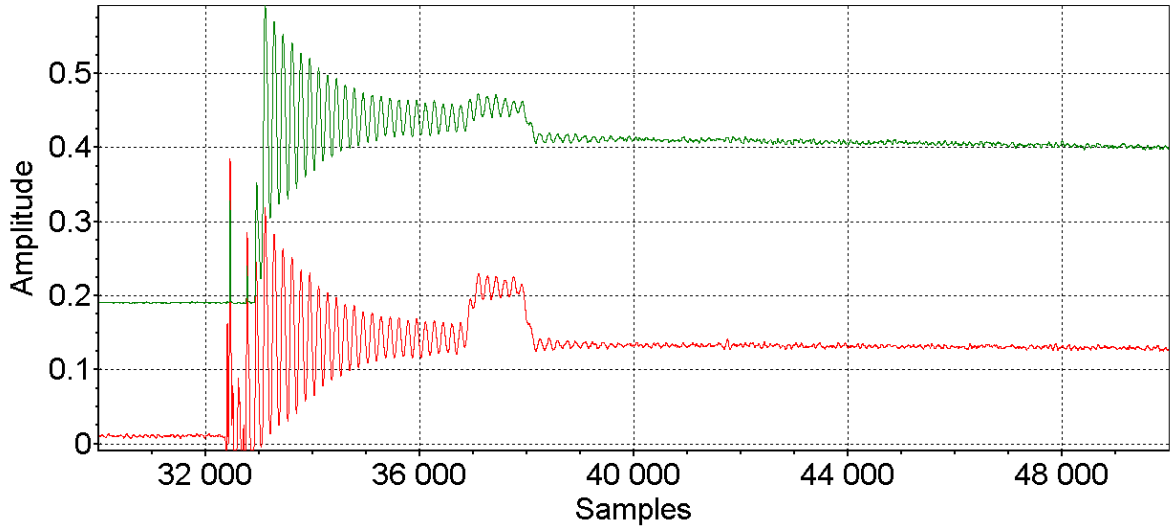

Figure 6. Stokes and anti-Stokes components at 97.2 °C arisen at 37000 sample.

4. Spatial resolution

The determined statistical characteristics of the signal should make it possible to reduce the number of target pulses for evaluation of temperature. It can be carried out empirically [16]. But the investigated approach will require calibration of the device if the statistical characteristics change for some reasons. Other methods of eliminating noise are much more complicated [17]. Therefore, it is necessary to control the average SD values of groups in order to well-timed correct coefficients of the calibration functions during operation. It can be fulfilled automatically with remote calibration protocol [18].

A refined estimate of the Stokes and anti-Stokes amplitudes makes possible to give a more accurate evaluation of the spatial position in the position with temperature difference and therefore, increase the spatial resolution. The approach is based on approximation of response by the potential characteristic of the linear filtering system [19–20]. Let signal on the linear filtering system input be

$$x(t) = \frac{1}{2} + \frac{2}{\pi} \sum_{k=1,3...}^{\infty} \frac{1}{k} \sin(\Omega_1 k t) \tag{2}$$

representing a rectangular wave. At the output of the system we have (figure 6):

$$y(t) = \frac{1}{2} + \frac{2}{\pi} \sum_{k=1,3...}^{2n+1} a_k \sin(\Omega_k \bar{t} + \varphi_k), \tag{3}$$

where $\Omega_k = (2\pi / \Omega_0 T)k$; $\Omega_{2n+1} = 1$; $\Omega_1 = 1/(2n+1)$; $\bar{t} = \omega_0 t$; ω_0 is normalized frequency. Target of the system is a trigonometric polynomial. Period T of the rectangular wave determines the number of terms and frequencies of harmonic components, and the coefficients a_k and φ_k is amplitude-frequency and phase-frequency characteristics of the system respectively. At a sufficiently large T, the system target approaches the transition characteristic of the ideal filtering system. From [20] it is known there is a single frequency response provides a potential transient response for the defined form of overshoot damping δ. In this case, the phase-frequency characteristic should be a linear function of frequency. The coefficients a_k were found for various δ. Figure 7 shows the potential transient characteristics and their corresponding amplitude-frequency characteristics at different overshoot δ.

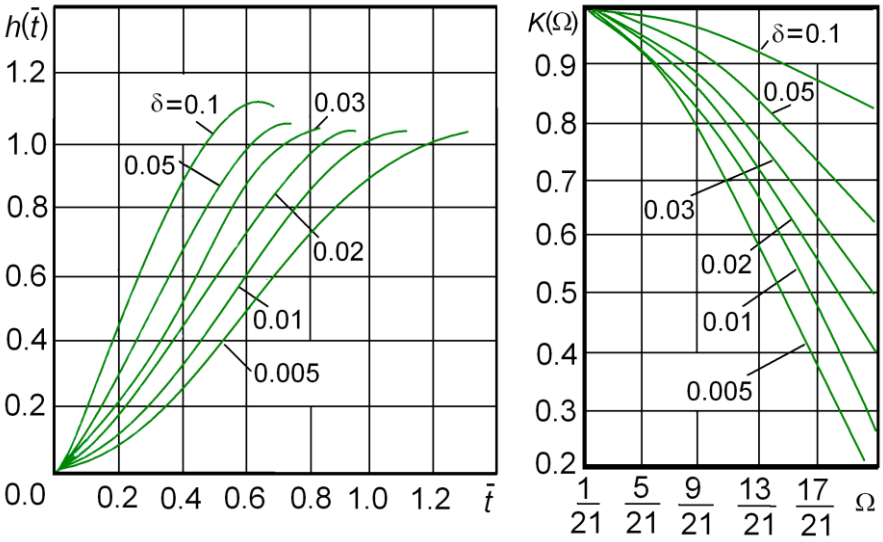

Figure 7. Potential transient response and corresponding amplitude-frequency characteristics at different overshoot δ.

Comparing figures 6 and 7, it can be assumed that the highest spatial resolution can be achieved with the largest δ since this value corresponds to the smallest risetime but it will require a wide spectrum. The frequency band can not be expanded reducing the gain. But for DTS this is not applicable due to the low signal-to-noise ratio. Unlike picosecond amplifiers, high overshoot is preferable and will require fewer approximation coefficients.

For DTS model it has been chosen n=3, thus coefficients are equal: a_1=1.271, a_3=0.41772. Value of peak overshoot was chosen δ=0.5 for the worst case. The arithmetic average was calculated:

$$S(\varepsilon) = \overline{[\varepsilon \cdot N_1(1)] \cdot h_1(t) + [\varepsilon \cdot N_2(1)] \cdot h_2(t)} \quad (4)$$

where N is normally distributed random variable with SD equal 1 and mean 0; ε=0.03 is noise level, $h_1(t)$ and $h_2(t)$ are potential transient characteristics 1 and 2 (see figure 8).

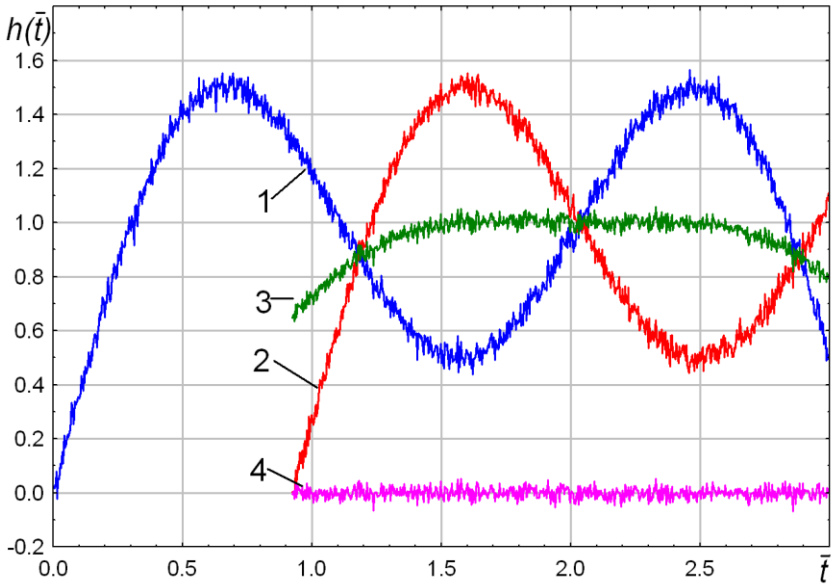

Figure 8. Potential transient response (1, 2) with noise, average transient response, and difference of the average transient with noise and average transient without noise (4).

SD for $\varepsilon \cdot N_1(1) = 0.03$, and for difference (4) it is equal to 0.01, i.e. three times less. It follows that the delay of samples by a time equal to a quarter of period of the wave function reduces the noise in three times.

5. Conclusion

The structure of DTS signals was studied, in which the temperature is calculated by extracting the Stokes and anti-Stokes components from the reflected light. Noise arising from transients and used elements influenced to the weak signals before amplification. It is proposed to evaluate the additive noise using the average SD when dividing the signal into groups. It was shown when the optimal grouping interval is determined, the SD in each group differs slightly. It confirms the supposition that this value can be used to estimate additive noise. To get rid of noise arising from the transient, it is proposed to reduce the operating area to the point where its effect becomes insignificant. Practice shows the transition process significantly increases the measurement error in this interval, which makes the measurements there less reliable. To increase the spatial resolution, the transition signal between different temperatures is presented as the potential characteristic of the linear filtering circuit. The model example shows that the delay of the samples of the potential transient response by a time equal to quarter of the period of the wave function reduces the noise by three times.

6. References

[1] W.P. Ng, N. Lalam, 2016, Future of Distributed Fiber Sensors (Invited Paper), 15th International Conference on Optical Communications and Networks (ICOCN).

[2] O.V. Stukach, I.V. Sychev, 2018, Signal Processing in the Distributed Temperature Sensors by Raman Backscatter: Review of New Outcomes, Radioengineering, no. 3, p. 86–92. - ISSN 0033-8486, http://www.radiotec.ru/number/1764.

[3] S. Wang, K. Lasn, C.W. Elverum, D. Wan, A. Echtermeyer, 2020, Novel in-situ residual strain measurements in additive manufacturing specimens by using the Optical Backscatter Reflectometry, Additive Manufacturing 32 (2020) 101040, DOI:10.1016/j.addma.2020.101040.

[4] Jian Li, Tao Yu, Mingjiang Zhang, Jianzhong Zhang, Lijun Qiao, Tao Wang, 2019 Temperature and Crack Measurement Using Distributed Optic-Fiber Sensor Based on Raman Loop Configuration and Fiber Loss, IEEE Photonics Journal, vol. 11, Issue 4. DOI: 10.1109/JPHOT.2019.2931306. https://ieeexplore.ieee.org/document/8777155.

[5] M. Yin, B. Gu, Q.F. An, C. Yang, Y.L. Guan, K.T. Yong, 2018, Recent development of fiber-optic chemical sensors and biosensors: Mechanisms, materials, micro/nano-fabrications and applications, Coordination Chemistry Reviews 376 (2018) 348-392, DOI: 10.1016/j.ccr.2018.08.001.

[6] E. Vorathin, Z.M. Hafizi., N. Ismail, M. Loman, 2020, Review of high sensitivity fibre-optic pressure sensors for low pressure sensing, Optics and Laser Technology, 121 (2020) 105841, DOI: 10.1016/j.optlastec.2019.105841.

[7] Yunli Dang, Zhiyong Zhao, Xuefeng Wang, Ruolin Liao, Chao Lu, 2019 Simultaneous Distributed Vibration and Temperature Sensing Using Multicore Fiber, IEEE Access, vol. 7. 10.1109/ACCESS.2019.2948213. https://ieeexplore.ieee.org/document/8876632.

[8] F. Zhao, R. Xue, J. Wang, Z. Zhang, K. Zhang, R. Chen, Y. Luo, S. Wang, 2020, A fiber optic temperature sensor based on interference fringe contrast demodulation, Optik - International Journal for Light and Electron Optics, 204 (2020) 164014, DOI: 10.1016/j.ijleo.2019.164014.

[9] J. Villatoro, D. Monzo_n-Herna_ndez and D. Talavera, 2004, High resolution refractive index sensing with cladded multimode tapered optical fibre, Electronics Letters, 22nd January, Vol. 40, No. 2.

[10] Dong Wang , Bizhao Cheng, Baoquan Jin, Yu Wang , Mingjiang Zhang, Xin Liu, and Qing Bai, 2019, Remote Simultaneous Measurement of Liquid Temperature and Refractive Index Using Fiber-Optic Spontaneous Raman Scattering, IEEE Sensors Journal, Vol. 19, No. 22,

November 15, 10513, DOI: 10.1109/JSEN.2019.2930108. https://ieeexplore.ieee.org/document/8767006.

[11] S F S M Noor et al, 2019 Multimode interference based fiber-optic sensor for temperature measurement, J. Phys.: Conf. Ser. 1151 012023.

[12] X. Fu, Y. Zhang, Y. Wang, G. Fu, W. Jin, W. Bi, 2020, A temperature sensor based on tapered few mode fiber long-period grating induced by CO2 laser and fusion tapering, Optics and Laser Technology 121 (2020) 105825, DOI: 10.1016/j.optlastec.2019.105825.

[13] X. Q. Lei, Y. Feng, X. P. Dong, High-temperature sensor based on a special thin-diameter fiber. 2020, Optics Communications 463 (2020) 125386. DOI: 10.1016/j.optcom.2020.125386.

[14] J. Jin, H. Zhang, Y. Guo, N. Song, 2020, Modeling and Optimization of a Cost-Efficient Distributed Temperature Sensor Based on Temperature Sensitive Optical Fibers, IEEE Sensors Journal Vol. 20, Issue 3, pp. 1306–1314. DOI: 10.1109/JSEN.2019.2946327. http://ieeexplore.ieee.org/document/8862906.

[15] Saiied M. Aminossadati, Nayeemuddin M. Mohammed, Javad Shemshad, 2010, Distributed temperature measurements using optical fibre technology in an underground mine environment, Tunnelling and Underground Space Technology 25(2010), p. 220–229, DOI: 10.1016/j.tust.2009.11.006, https://www.elsevier.com/locate/tust.

[16] M.K.Saxena, S.D.V.S.J. Raju, R. Arya, R.B.Pachori, S.V.G. Ravindranath, S. Kher, and S.M. Oak, 2016, Empirical Mode Decomposition-Based Detection of Bend-Induced Error and Its Correction in a Raman Optical Fiber Distributed Temperature Sensor, IEEE Sensors Journal, vol. 16, No. 5, p. 1243-1252. DOI: 10.1109/JSEN.2015.2499242.

[17] L. Pan, K. Liu, J. Jiang, C. Ma, M. Tian, and T. Liu, 2017, A De-Noising Algorithm Based on EEMD in Raman-Based Distributed Temperature Sensor, IEEE Sensors Journal, vol. 17, No. 1, January 1, p.134–138. DOI: 10.1109/JSEN.2016.2623860.

[18] Raushan Zh. Aimagmbetova, Ivan A. Ershov, Oleg V. Stukach. "Towards the problem of measurement traceability in the Internet of measurement concept". Dynamics of Systems, Mechanisms and Machines (Dynamics), Conference, Omsk, 14-16 Nov. 2017. ISBN: 978-1-5386-1820-2. DOI: 10.1109/Dynamics.2017.8239425. http://ieeexplore.ieee.org/document/8239425/.

[19] J.P. Bazzo, D.R. Pipa, C. Martelli, E. Vagner da Silva, and J.C.Cardozo da Silva, 2016 Improving Spatial Resolution of Raman DTS Using Total Variation Deconvolution, IEEE Sensors Journal, vol.16, NO. 11, JUNE 1, p. 4425–4430. DOI: 10.1109/JSEN.2016.2539279.

[20] Oleg V. Stukach, Ivan A. Ershov, Igor V. Sychev 2018 Towards the Distributed Temperature Sensor with Potential Characteristics of Accuracy, XIV International Scientific-Technical Conference on Actual Problems of Electronics Instrument Engineering (APEIE), October 2-6, 2018, Novosibirsk, Russia. DOI: 10.1109/APEIE.2018.8546271.

Acknowledgments

Authors would like to thank NETI leadership for their support and feedback. This study has been funded by Russian Foundation for Basic Research according to the research project N 20-08-00321.